



## Research Article

Niko Guskos, Grzegorz Zolnierkiewicz\*, Aleksander Guskos, Konstantinos Aidinis, Agnieszka Wanag, Ewelina Kusiak-Nejman, Urszula Narkiewicz, and Antoni W. Morawski

# Magnetic moment centers in titanium dioxide photocatalysts loaded on reduced graphene oxide flakes

<https://doi.org/10.1515/rams-2021-0012>

Received Sep 09, 2020; accepted Nov 19, 2020

**Abstract:** A whole series of titania nanocomposites modified with reduced graphene oxide (rGO) was prepared using solvothermal method followed by calcination. Modification of titania with rGO has been found to lead to better photocatalytic properties. The highest photocatalytic performance was obtained at calcination temperature of 600°C. Electron paramagnetic resonance/ferromagnetic resonance measurements showed oxygen defects and ferromagnetic ordering systems. The linewidth of resonance line of oxygen defects decreased linearly with calcination temperature increasing up to 600°C and an accompanying growth of mean crystallite size of anatase phase. The integrated resonance line intensity of oxygen defects depended on the calcination temperature and caused a very large increase in the intensity of resonance lines originating from oxygen defects, because inert atmosphere of calcination was enhanced by graphene presence. The occurrence of magnetic ordering system significantly influenced the performance of photocatalytic processes by changing the amount of oxygen defects.

**Keywords:** Magnetic oxygen defects and ferromagnetic ordering systems, Titania nanocomposites modified with reduced graphene oxide (rGO), Electron paramagnetic resonance/ferromagnetic resonance

## 1 Introduction

Recently, several papers about studies of graphene oxide (GO) and reduced graphene oxide (rGO) nanomaterials using magnetic resonance method appeared [1–4]. The preparation and application of titanium dioxide nanomaterials modified with carbon have been intensively studied [5–10]. For years, modified titanium dioxide has been and is being investigated by magnetic resonance method *e.g.* [11–22]. The method enables to study localized magnetic moments associated with resulting defects that play an important role in various properties useful in many processes, including catalysis and photocatalysis. In the abundant literature concerned photocatalysis with using of TiO<sub>2</sub>-graphene hybrids we found a limited number of publications on relation of the photoactivity and the amount of magnetic moment centres. This problem is especially interesting in TiO<sub>2</sub>-graphene system with interphases created under elevated temperatures and under inert argon atmosphere. Therefore in this work we have undertaken study on this matter.

The main aim of the work was to prepare a series of TiO<sub>2</sub>-rGO nanocomposites at different treatment temperatures and study of localized magnetic moments together with correlated spin systems using the method of Electron Paramagnetic Resonance/Ferromagnetic Resonance (EPR/FMR).

Magnetic oxygen defects or magnetic agglomerates significantly affect photocatalytic processes even though they are in a small amount then it is important to concentrate them properly.

**\*Corresponding Author: Grzegorz Zolnierkiewicz:** Department of Technical Physics, West Pomeranian University of Technology in Szczecin, Al. Piastow 48, 70-311 Szczecin, Poland;  
Email: grzegorz.zolnierkiewicz@zut.edu.pl

**Niko Guskos, Aleksander Guskos:** Department of Technical Physics, West Pomeranian University of Technology in Szczecin, Al. Piastow 48, 70-311 Szczecin, Poland

**Konstantinos Aidinis:** Department of Electrical Engineering, Ajman University of Science and Technology, PO Box 346, Ajman, United Arab Emirates

**Agnieszka Wanag, Ewelina Kusiak-Nejman, Urszula Narkiewicz, Antoni W. Morawski:** Department of Inorganic Chemical Techno-

logy and Environment Engineering, West Pomeranian University of Technology in Szczecin, Pułaskiego 10, 70-322 Szczecin, Poland



## 2 Experimental

### 2.1 Materials

The crude titanium dioxide provided by the Chemical Plant Grupa Azoty Zakłady Chemiczne “Police” S.A. (Poland) was used as a starting material for preparing a new group of photocatalysts. The supplied titanium dioxide was pre-treated as was described elsewhere [23]. The sample after pre-treatment was named as starting-TiO<sub>2</sub>. Reduced graphene oxide was obtained by NANOMATERIALS LS (Poland) using a modified Hummers’ method.

### 2.2 Preparation of photocatalysts

The graphene modified TiO<sub>2</sub> photocatalysts were obtained by solvothermal process at temperature of 180°C (sample name as TiO<sub>2</sub>-A180), mixing with graphene, and then calcination. The starting solvothermal TiO<sub>2</sub> was mechanically mixed with 8 wt% of rGO and then placed in autoclave with isopropanol. The sample was heated at 180°C for 4 h under autogenous pressure. The sample after this modification was named as TiO<sub>2</sub>/rGO-8 and was also used as a control material. Then, TiO<sub>2</sub>/rGO-8 photocatalyst was calcined at 400°C, 500°C, 600°C and 800°C for 4 h in an argon flow. The obtained materials were named as TiO<sub>2</sub>/rGO-8-400, TiO<sub>2</sub>/rGO-8-500, TiO<sub>2</sub>/rGO-8-600 and TiO<sub>2</sub>/rGO-8-800.

### 2.3 Photocatalytic activity measurements

The photocatalytic activity was investigated using the acid blue decomposition as a model reaction. The photocatalytic reaction was performed in a glass beaker (0.3 L) containing 0.8 g/L of photocatalyst and 0.2 L of pollutant solution. The initial concentration of acid blue was 10 mg/L. The suspension was stirred in darkness to reach the adsorption-desorption equilibrium. After that, the solution was irradiated using UV-Vis light with high UV intensity (UV irradiation).

### 2.4 Characterization of photocatalysts

The phase composition and crystal structure were analyzed using the method of powder X-ray diffraction (XRD) analysis (Malvern PANalytical Ltd., Netherlands) with Cu K $\alpha$  radiation ( $\lambda = 1.54056 \text{ \AA}$ ). The anatase and rutile concentration and the average crystallite size of anatase were calculated by the method described elsewhere [24]. EPR mea-

surements were carried out on Bruker E 500 spectrometer operating at X-band microwave frequency. Temperature studies at 90 K and 290 K were performed using an Oxford ESP 300 continuous flow cryostat. The investigated sample was in form of loose powder and during the measurements it was placed in a quartz tube.

## 3 Results and discussion

From data presented in Figure 1 we can conclude that incorporation of graphene to TiO<sub>2</sub> and further calcination of graphene modified TiO<sub>2</sub> in argon atmosphere enabled to create a new structure of hybrid TiO<sub>2</sub>-rGO materials, which exhibited much higher photoactivity under UV radiation for acid blue decomposition than TiO<sub>2</sub> sample.

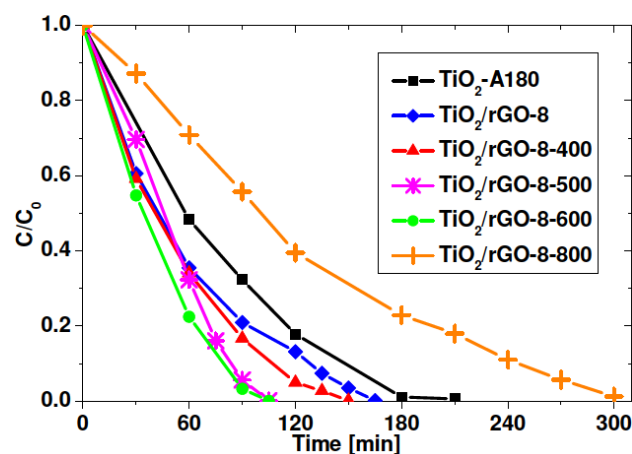


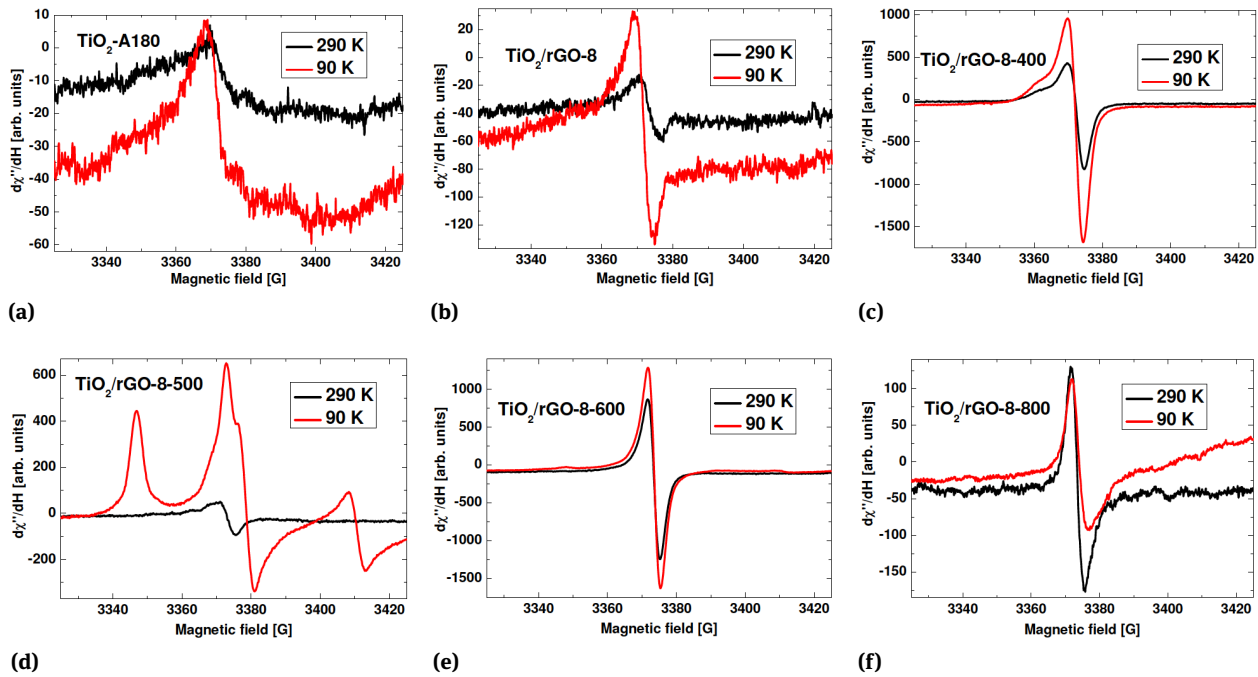
Figure 1: Acid blue decomposition degree under UV light irradiation

The total time of complete removal of acid blue decreased from 210 min for TiO<sub>2</sub>, to 165 min for TiO<sub>2</sub>/rGO-8, 150 min for TiO<sub>2</sub>/rGO-400 and 105 min for TiO<sub>2</sub>/rGO-8-600 photocatalysts. The photocatalyst heated at 800°C showed a lower photoactivity, almost 300 min removal of acid blue, in comparison to the references TiO<sub>2</sub> and other obtained samples. This behavior could be considered with the phase composition presented in Table 1.

The samples of higher photoactivity still kept a low content of rutile and high content of crystalline phase of anatase (96-99%) with low mean crystallite size of anatase, between 17-29 nm. The sample TiO<sub>2</sub>/rGO-8-800 contained mainly rutile phase (97%) with high mean crystallite size (over 100 nm) which was characterized by lower photoactivity in comparison to anatase phase, which was of low contribution in composition as well as of higher mean crystallite size of 65 nm. This simultaneous effect of shifting sizes

**Table 1:** XRD phase composition and mean crystallites size of reference, control and obtained photocatalysts

Sample code	Concentration of anatase phase %	Concentration of rutile phase %	Mean size of anatase crystallite [nm]	Mean size of rutile crystallite [nm]
TiO <sub>2</sub> -A180	98	2	18	33
TiO <sub>2</sub> /rGO-8	99	1	17	27
TiO <sub>2</sub> /rGO-8-400	98	2	19	29
TiO <sub>2</sub> /rGO-8-500	96	4	22	56
TiO <sub>2</sub> /rGO-8-600	97	3	29	40
TiO <sub>2</sub> /rGO-8-800	3	97	65	>100

**Figure 2:** The EPR spectra of nanocomposites at 90 K (red) and 290 K (black): (a) TiO<sub>2</sub>-A180, (b) TiO<sub>2</sub>/rGO-8, (c) TiO<sub>2</sub>/rGO-8-400, (d) TiO<sub>2</sub>/rGO-8-500, (e) TiO<sub>2</sub>/rGO-8-600 and (f) TiO<sub>2</sub>/rGO-8-800

from nanometers to almost micrometers for rutile caused an additional negative effect on photoactivity. High photocatalytic performance was obtained for the TiO<sub>2</sub>/rGO-400, TiO<sub>2</sub>/rGO-8-500 and TiO<sub>2</sub>/rGO-8-600 nanocomposites (Figure 1).

Figure 2 presents the EPR spectra for the all nanocomposites at 90 K and 290 K.

A narrow resonance line was observed in all nanocomposites and fitted using the Lorentzian function. All lines had almost the same  $g$  parameter value ( $g = 2.0033$  (1)). A similar line was observed for rGO [2–4]. The values of linewidth  $\Delta H$  at 90 K and 290 K are shown in Figure 3.

At both temperatures, the linewidth of the resonance lines decreased up to a minimum for the TiO<sub>2</sub>/rGO-8-600 sample and then a pronounced increase for TiO<sub>2</sub>/rGO-8-

800 sample. Spin relaxation processes significantly depend on calcination temperature. Additionally, an intense anisotropic EPR powder spectrum with rhombic  $g$ -tensor ( $g_x = 1.98$ ,  $g_y = 2.00$  and  $g_z = 2.02$ ) was observed for sample TiO<sub>2</sub>/rGO-8-500 (arising from oxygen defect associated with trivalent titanium ions) similar as TiO<sub>2</sub> [2]. Much lower intensity of these lines occurred in the nanocomposite TiO<sub>2</sub>/rGO-8-600.

Figure 4 shows the integrated intensity ( $I_{int} = A \cdot \Delta H^2$ ,  $A$  – signal amplitude and  $\Delta H$  – linewidth) at 90 K and 290 K.

The normalized integrated intensity gives us the amount of localized magnetic centers, but the presence of conducting electrons especially at high temperatures could change them by skin effect [25]. The skin depth  $\delta$  for microwave radiation varied inversely proportional to the

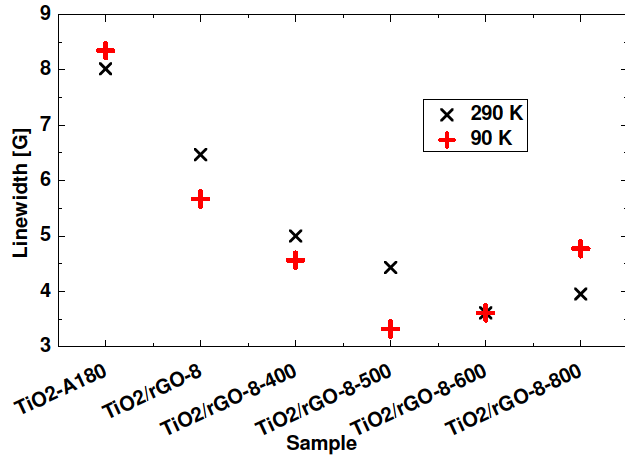


**Figure 3:** The linewidth  $\Delta H$  of the narrow resonance line in different samples measured at 90 K and 290 K

sample conductivity which led to a reduction of the EPR line intensity through an effective decrease of the active volume of the sample. The samples TiO<sub>2</sub>/rGO-8-400 and TiO<sub>2</sub>/rGO-8-600 showed the highest intensities of the resonance line arising from oxygen defects (free radicals) at 90 K. The narrow resonance line intensity in rGO increased and diminished reversibly with potential [4]. As a result of this process, we can have electron transfer reducing their number in the conduction band and thus increasing the volume of penetration of microwave radiation at 290 K. From Figure 1 it can be seen that the photoactivity under UV irradiation increased with the increase of calcination temperature to 600°C. The rutile phase was dominating in the TiO<sub>2</sub>/rGO-8-800 nanocomposite, hence the activity was much weaker than that of other materials. The oxygen defects may be one of the causes of electron transfer. Additional oxygen defects in the right proportion quantities improved some photocatalytic properties. The significant reduction in the number of oxygen defects associated with trivalent titanium ions change slowly the photocatalytic properties from nanocomposites TiO<sub>2</sub>/rGO-8-500 to TiO<sub>2</sub>/rGO-8-600.

Additional magnetic resonance spectra are observed in the low magnetic field (Figure 5), but they are not visible at 90 K.

Low magnetic concentration of nanoagglomerates in non-magnetic matrices with a decrease at lower temperature become less visible [26]. For nanocomposites TiO<sub>2</sub>-A180, TiO<sub>2</sub>/rGO-8-400, TiO<sub>2</sub>/rGO-8-500 and TiO<sub>2</sub>/rGO-8-800, the resonance line are fitted with one Lorentzian function. For nanocomposite TiO<sub>2</sub>/rGO-8 the resonance lines are fitted with three Lorentzian functions and in nanocomposite TiO<sub>2</sub>/rGO-8-600 they are fitted by two Lorentzian functions. Table 2 shows the results obtained from fitting of the spectra derived from magnetic ordering systems.

In TiO<sub>2</sub> we have one magnetic ordering system with lowest integrated intensity (Table 2). The nanocomposite TiO<sub>2</sub>/rGO-8 exhibited three magnetic ordering systems. Two are from phase anatase and one is probably from the rutile phase (comparable in intensity to the nanocomposite TiO<sub>2</sub>/rGO-8-800). The total intensity value in the TiO<sub>2</sub>/rGO-8 is comparable to the TiO<sub>2</sub>/rGO-8-400 nanocomposite (Table 2). In the nanocomposites processed at calcining temperature 400°C and 600°C the resonance line intensity resulting from oxygen defects associated with free radicals increased quite significantly (Figure 4). The total intensity from ordered magnetic moments for TiO<sub>2</sub>/rGO-8-600 increased 4.5 times to TiO<sub>2</sub>/rGO-8-400. In the TiO<sub>2</sub>/rGO-8-500 nanocomposite, the number of oxygen defects related to trivalent titanium ions increased significantly (Figure 2d) and the number of ordering magnetic moments decreased (Table 2). Localized magnetic moments from trivalent titanium ions at a calcination temperature of 600°C can create ordered magnetic moments of smaller sizes compared to other nanocomposites.

The TiO<sub>2</sub>/rGO-8 sample also showed a wider resonance line described at  $H=3360$  G [3] which did not occur in the remaining nanocomposites.

In the case of a larger number of magnetic ions, the resonance field is many times further shifted towards the lower applied magnetic field [27]. The resonance condition

**Table 2:** The resonance field ( $H$ ), linewidth ( $\Delta H$ ) and integrated intensity ( $I$ ) (related to the second sample) for broad line

Sample code	H(1) [G]	$\Delta H(1)$ [G]	I(1)	H(2) [G]	$\Delta H(2)$ [G]	I(2)
TiO <sub>2</sub> -A180	3122(6)	451(7)	0.64			
TiO <sub>2</sub> /rGO-8	1826(3)	307(3)	1.00	2561(2)	171(5)	0.26
	3064(17)	515(14)	1.48			
TiO <sub>2</sub> /rGO-8-400	3106(10)	563(14)	2.96			
TiO <sub>2</sub> /rGO-8-500	3180(6)	475(8)	1.1			
TiO <sub>2</sub> /rGO-8-600	2944(40)	724(27)	9.42	2136(10)	420(14)	4.05
TiO <sub>2</sub> /rGO-8-800	3092(7)	506(9)	1.23			

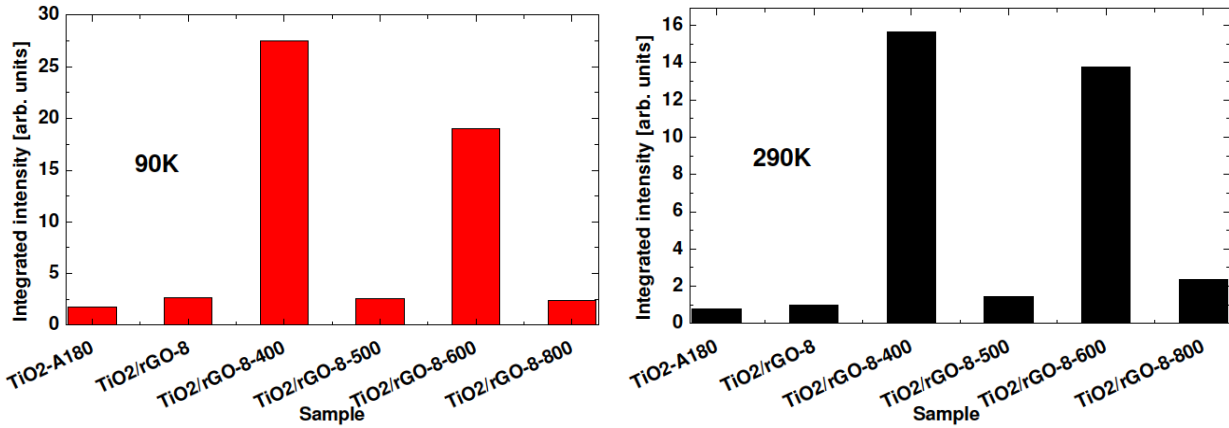


Figure 4: Integrated intensities the EPR spectra of defects arising from oxygen defects at 90 K and 290 K

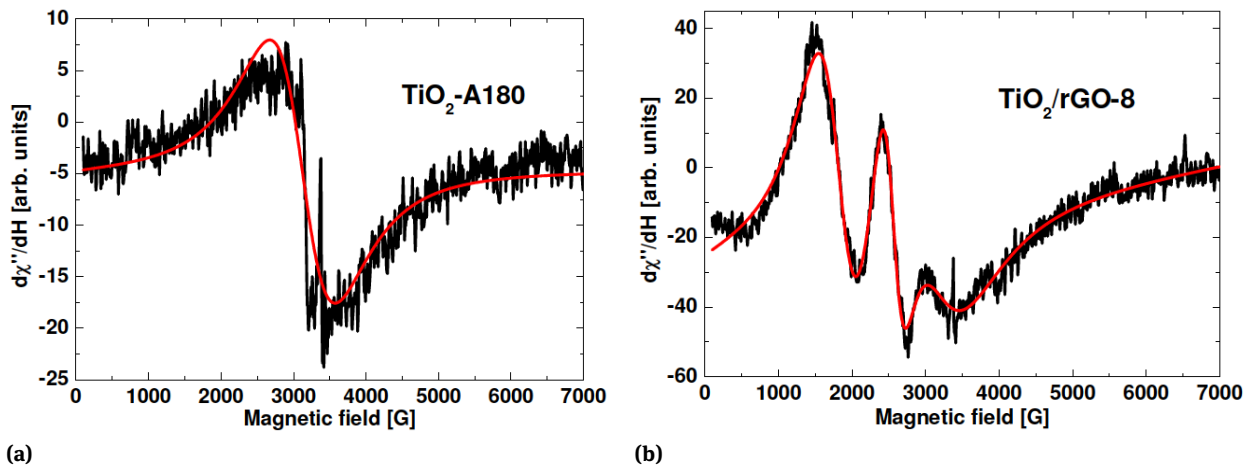


Figure 5: EPR spectra of the nanocomposites at low magnetic field: a) sample TiO<sub>2</sub>-A180 and b) nanocomposite TiO<sub>2</sub>/rGO-8

is the following:  $h \cdot \nu = g_{eff} \cdot \mu_B \cdot (H_o - H_r)$ , where  $h$  and  $\mu_B$  are Planck and Bohr magneton constants, respectively  $H_o$  – external applied magnetic field and  $H_r$  – internal magnetic field, where the values of resonance field  $H_o - H_r$  are shown in the Table 2. The observed magnetic resonance signal could be regarded as a ferromagnetic one.

Magnetic ordering system formed on the basis of trivalent titanium ions, at a calcination temperature of 400°C passed into localized magnetic moments oxygen defects for nanocomposite TiO<sub>2</sub>/rGO-8-500. The magnetic ordering system at higher calcining temperature caused a rapid increase in oxygen defect both associated with free radicals and titanium trivalent ions.

Most oxygen defects (free radicals) were observed for the TiO<sub>2</sub>/rGO-8-400 and TiO<sub>2</sub>/rGO-8-600 nanocomposites. The highest amount of oxygen defects associated with trivalent titanium ions was achieved for the TiO<sub>2</sub>/rGO-8-500 nanocomposite. A significantly faster increase of free radicals at 290 K for TiO<sub>2</sub>/rGO-8-600 nanocomposite can be

seen in Figure 4. It is probably related to a greater amount of conductivity electrons in the TiO<sub>2</sub>/rGO-8-400 nanocomposite. Coexistence in appropriate proportions of magnetic ordering systems and oxygen defects can significantly improve photocatalytic performance.

## 4 Conclusions

A whole series of TiO<sub>2</sub> nanocomposites modified with rGO was prepared using a solvothermal method followed by calcination. It was found that modification of TiO<sub>2</sub> with rGO significantly improved photocatalytic properties. The highest photocatalytic efficiency was achieved for the nanocomposite calcined at 600°C. Spectra of EPR/FMR at 90 K and 290 K showed oxygen defects and ferromagnetic ordering system connected with trivalent titanium ions. The linewidth of the resonance lines decreased almost linearly for the

nanocomposites with a higher crystallite size of anatase phase caused by increasing calcination temperature.

The following essential conclusions can be drawn:

- relaxation spin processes significantly depended on the calcination temperature of the composite samples,
- magnetic ordering system indirectly significantly influenced photocatalytic performance,
- for TiO<sub>2</sub>/rGO-8-400 and TiO<sub>2</sub>/rGO-8-600 nanocomposites, the magnetic resonance line from magnetic ordering system and the integrated intensity of the resonance lines from oxygen defects (free radicals) drastically increased,
- EPR spectrum of resonance lines from titanium trivalent ions in TiO<sub>2</sub>/rGO-8-500 nanocomposite increased significantly that positively effected on photocatalytic processes.
- In TiO<sub>2</sub>/rGO-8-600 nanocomposite, a significant increase in ordering magnetic systems associated with a decrease in size was noticed

**Author Contribution:** N. Guskos: Visualization, Conceptualization, Methodology, Writing- Original Draft, Supervision  
G. Zolnierkiewicz, A. Guskos: Data curation, Investigation

K. Aidinis: Software, Validation

A. Wanag, E. Kusiak-Nejman: Methodology, Conceptualization, Writing- Original Draft

U. Narkiewicz: Writing- Original Draft, Supervision, Funding acquisition

A. W. Morawski: Visualization, Conceptualization, Writing- Original Draft, Supervision,

**Conflict of Interests:** The authors declare that they have no known competing financial interests or personal relationships that could have appeared to influence the work reported in this paper.

**Data availability statement:** All data generated or analyzed during this study are included in this published article or are available from the corresponding author on reasonable request.

**Acknowledgement:** The research leading to these results has received funding from the Norway Grants 2014-2021 via the National Centre for Research and Development under the grant no. NOR/POLNORCCS/PhotoRed/0007/2019-00.

## References

- [1] Kempinski, M., S. Łos, P. Florczak, W. Kempinski, and S. Jurga. EPR and impedance measurements of graphene oxide and reduced graphene oxide. *Acta Physica Polonica A*, Vol. 132, No. 1, 2017, pp. 81–85.
- [2] Diamantopoulou, A., S. Glenis, G. Zolnierkiewicz, N. Guskos, V. Likodimos. Magnetism in pristine and chemically reduced graphene oxide, *Journal of Applied Physics* 121 (2017) 043906 pp. 1-11.
- [3] Wang, B., V. Likodimos, A. J. Fielding, and R. A. W. Dryfe. In situ electron paramagnetic resonance spectroelectrochemical study of graphene-based supercapacitors: Comparison between chemically reduced graphene oxide and nitrogen-doped reduced graphene oxide. *Carbon*, Vol. 160, 2020, pp. 236–246.
- [4] Wang, B., A. J. Fielding, and R. A. W. Dryfe. Electron paramagnetic resonance as a structural tool to study graphene oxide: Potential dependence of the EPR response. *Journal of Physical Chemistry C*, Vol. 123, No. 36, 2019, pp. 22556–22563.
- [5] Liu, F., X. Shao, J. Wang, S. Yang, H. Li, X. Meng, X. Liu, and M. Wang. Solvothermal synthesis of graphene-CdS nanocomposites for highly efficient visible-light photocatalyst. *Journal of Alloys and Compounds*, Vol. 551, 2013, pp. 327–332.
- [6] Hu, C., T. Lu, F. Chen, and R. Zhang. A brief review of graphene-metal oxide composites synthesis and applications in photocatalysis. *Journal of the Chinese Advanced Materials Society*, Vol. 1, No. 1, 2013, pp. 21–39.
- [7] Ji, T., M. Sun, and P. Han. A review of the preparation and applications of graphene/semiconductor composites. *Carbon*, Vol. 70, 2014, pp. 319–322.
- [8] Okoth, O. K., K. Yan, and J. Zhang. Mo-doped BiVO<sub>4</sub> and graphene nanocomposites with enhanced photoelectrochemical performance for aptasensing of streptomycin. *Carbon*, Vol. 120, 2017, pp. 194–202.
- [9] Kong, L. B., F. Boey, Y. Huang, Z. J. Xu, K. Zhou, S. Li, W. Que, H. Huang, and T. Zhang. Graphene-inorganic hybrids (I). In *Carbon nanomaterials based on graphene nanosheets*, 1st Edition (L. B. Kong, ed.), CRC Press, Boca Raton, FL, 2017, pp. 111–220.
- [10] Kusiak-Nejman, E., D. Moszynski, J. Kapica-Kozar, A. Wanag, Antoni W. Morawski, Assessment of the suitability of the one-step hydrothermal method for preparation of non-covalently/covalently-bonded TiO<sub>2</sub>/graphene-based hybrids, *Nanomaterials* 8(9) (2018) 647 pp. 1-17.
- [11] Naccache, C., P. Meriaudeau, M. Che, and A. J. Tench. Identification of oxygen species adsorbed on reduced titanium dioxide. *Transactions of the Faraday Society*, Vol. 67, 1971, pp. 506–512.
- [12] Serwicka, E., M. W. Schlierkamp, and R. N. Schindler. Localization of conduction band electrons in polycrystalline TiO<sub>2</sub> studied by ESR. *Zeitschrift für Naturforschung. Section A. Physical Sciences*, Vol. 36, No. 3, 1981, pp. 226–232.
- [13] Di Valentin, C., K.M. Neyman, T. Risse, M. Sterrer, E. Fischbach, H.J. Freund, V.A. Nasluzov, G. Pacchioni, N. Rösch, Density-functional model cluster studies of EPR g tensors of F+s centers on the surface of MgO, *The Journal of Chemical Physics*, Vol. 124, 2006, id 044708.
- [14] Ciric, L., A. Sienkiewicz, D. M. Djokic, R. Smajda, A. Magrez, T. Kaspar, R. Nesper, and L. Forro. Size dependence of the magnetic response of graphite oxide and graphene flakes – an electron spin resonance study. *Physica Status Solidi. B, Basic Research*,

- Vol. 247, No. 11-12, 2010, pp. 2958–2961.
- [15] Guskos, N., A. Guskos, J. Typek, P. Berczynski, D. Dolat, B. Grzmil, and A. Morawski. Influence of annealing and rinsing on magnetic and photocatalytic properties of TiO<sub>2</sub>. *Materials Science and Engineering B*, Vol. 177, No. 2, 2012, pp. 223–227.
- [16] Panich, A.M., A.I. Shames, N.A. Sergeev, M Olszewski, J.K. McDonough, V.N. Mochalin, Y. Gogotsi, Nanodiamond graphitization: a magnetic resonance study, *Journal of Physics: Condensed Matter*, Vol. 25, 2013, id. 245303.
- [17] Likodimos, V., A. Chrysi, M. Calamiotou, C. Fernández-Rodríguez, J. M. Dona-Rodríguez, D. D. Dionysiou, and P. Falaras. Microstructure and charge trapping assessment in highly reactive mixed phase TiO<sub>2</sub> photocatalysts. *Applied Catalysis B: Environmental*, Vol. 192, 2016, pp. 242–252.
- [18] Tryba, B., M. Wozniak, G. Zolnierkiewicz, N. Guskos, A. Morawski, C. Colbeau-Justin. Influence of an electronic structure of N-TiO<sub>2</sub> on its photocatalytic activity towards decomposition of acetaldehyde under UV and fluorescent lamps irradiation, *Catalysts*, Vol. 8, 2018, id. 85(1-18).
- [19] Nair, R.V., P.K. Gayathri, V.S. Gummaluri, P.M.G. Nambissan, C. Vijayan. Large bandgap narrowing in rutile TiO<sub>2</sub> aimed towards visible light applications and its correlation with vacancy-type defects history and transformation, *Journal of Physics D: Applied Physics*, Vol. 51, 2018, id. 045107.
- [20] Tampieri F. and A. Barbon, Chapter 2, Resolution of EPR signals in graphene-based materials from few layers to nanographites. In: Savchenko, D., and A. H. Kassiba. Editors. *Frontiers in Magnetic Resonance*, Published by Bentham Science Publishers, Sharjah, U.A.E., Vol. 1, 2018, pp. 36-66. <https://doi.org/10.2174/97816810869341180101>.
- [21] Typek, J., N. Guskos, G. Zolnierkiewicz, M. Pilarska, A. Guskos, E. Kusiak-Nejman, et al. Magnetic properties of TiO<sub>2</sub>/graphitic carbon nanocomposites. *Reviews on Advanced Materials Science*, Vol. 58, No. 1, 2019, pp. 107–122.
- [22] Augustyniak-Jabłokow, M. A., K. Tadyszak, R. Strzelczyk, R. Fedaruk, and R. Carmieli. Slow spin relaxation of paramagnetic centers in graphene oxide. *Carbon*, Vol. 152, 2019, pp. 98–105.
- [23] Kusiak-Nejman, E., A. Wanag, J. Kapica-Kozar, and A. W. Morawski. Preparation and characterisation of TiO<sub>2</sub> thermally modified with cyclohexane vapours. *International Journal of Materials & Product Technology*, Vol. 52, No. 3/4, 2016, pp. 286–297.
- [24] Janus, M., J. Zatorska, K. Zając, E. Kusiak-Nejman, A. Czyżewski, and A. W. Morawski. The mechanical and photocatalytic properties of modified gypsum materials. *Materials Science and Engineering B*, Vol. 236-237, 2018, pp. 1–9.
- [25] Guskos, N., G. P. Triberis, M. Calamiotou, Ch. Trikalinos, A. Koufoudakis, C. Mitros, et al. Temperature dependence of the EPR spectra of GdBa<sub>2</sub>Cu<sub>3</sub>O<sub>7-δ</sub> orthorhombic and tetragonal compounds with impurity phases. *Physica Status Solidi. B, Basic Research*, Vol. 163, No. 2, 1991, pp. K89–K94.
- [26] Guskos, N., V. Likodimos, S. Glenis, J. Typek, M. Maryniak, Z. Roslaniec, et al. Matrix effects on the magnetic properties of γ-Fe<sub>2</sub>O<sub>3</sub> nanoparticles dispersed in a multiblock copolymer, *Journal of Applied Physics*, Vol. 99, 2006, id. 084307(1-7).
- [27] Narkiewicz, U., N. Guskos, W. Arabczyk, J. Typek, T. Bodziony, W. Konicki, et al. XRD, TEM and magnetic resonance studies of iron carbide nanoparticle agglomerates in a carbon matrix. *Carbon*, Vol. 42, No. 5-6, 2004, pp. 1127–1132.